ORIGINAL PAPER

M. P. Rowe · C. L. Baube · E. R. Loew · J. B. Phillips

Optimal mechanisms for finding and selecting mates: how threespine stickleback (*Gasterosteus aculeatus*) should encode male throat colors

Abstract Male threespine stickleback (*Gasterosteus aculeatus*) use nuptial colors to attract mates and intimidate rivals. We quantified stickleback color and environmental lighting using methods independent of human perception to evaluate the information transmitted by male signals in a habitat where these signals are displayed. We also developed models of chromatic processing based on four cone photopigments (peak absorptions at 360, 445, 530, and 605 nm) characterized microspectrophotometrically in *G. aculeatus* and three other stickleback species. We show that a simple opponent mechanism receiving equally weighted inputs from cones with peak absorptions at 445 nm and 605 nm efficiently encodes variation in male throat colors. An orthogonal opponent mechanism—the difference between outputs of 530-nm cones and mean of outputs of 445- and 605-nm cones—produces a neural signal that could be used for species recognition and would be largely insensitive to variation in male throat color. We also show that threespine stickleback throats/photopigments are optimized for this coding scheme. These and other findings lead to testable hypotheses about the spectral processing mechanisms present in the threespine stickleback visual systems and the evolutionary interactions that have shaped this signal/receiver system.

M. P. Rowe (✉)
Neuroscience Research Institute and Department of Psychology,
University of California,
Santa Barbara, CA 93106, USA
E-mail: rowe@psych.ucsb.edu
Tel.: +1-805-8932446
Fax: +1-805-8934303

C. L. Baube
Department of Biology,
Oglethorpe University

E. R. Loew
Department of Biomedical Sciences,
Cornell University

J. B. Phillips
Biology Department,
Virginia Tech

Introduction

The goal of this paper is to contribute to a better understanding of how animals, particularly the threespine stickleback (*Gasterosteus aculeatus*), use color when signaling in their natural habitat. When studying visual signaling, researchers must distinguish between their own perceptions and those of their subjects (Bennett et al. 1994; Fleishman et al. 1998; Fleishman and Endler 2000) and take into account the environment in which signaling takes place (Endler 2000). The visibility and conspicuousness of signals depend in part upon illumination, transmission properties of media intervening between signalers and receivers, and spectral properties of the background. Not surprisingly, at least some animals are adapted to the specific photic conditions under which signaling occurs (e.g., Reimchen 1989; Boughman 2001, Gamble et al. 2003). Here we describe quantitative measurements of variation in spectral reflectance (color) among male threespine stickleback from a single breeding population, the lighting conditions at the time and place where this population breeds, and the spectral sensitivities of the animals' photoreceptors. We then use these measurements to develop models of the stickleback visual system's responses to male throat coloration so that we might gain insight into the functional relationships that influenced the potential coevolution of this signal/receiver system.

The visual problems

Anadromous populations of stickleback migrate into brackish tidal pools to reproduce. The fitness of an

individual from such a population will depend, in part, on its ability to detect, identify, and discriminate among conspecifics in these pools. Fish may use different sets of cues to (1) detect that *something* is there, (2) identify whether or not that something is a conspecific male stickleback, and (3) discriminate differences in quality among identified male stickleback. Males, as the principle signalers, may similarly benefit from being detected by other stickleback, correctly identified as conspecific males, and (if cheating is costly) accurately assessed.

For the breeding season, male stickleback in many populations produce striking nuptial coloration patterns consisting—in human perceptual terms—of a bright blue-green iris and a reddish throat. A variety of studies suggest that nuptial coloration plays an important role in stickleback behavioral ecology (reviewed in Rowland 1994). Male stickleback judged by human observers to be more colorful—primarily based on the degree of throat "redness"—are more attractive to females (e.g., Ter Pelkwijk and Tinbergen 1937; Bakker 1993) and more successful in agonistic encounters with other males (e.g., Östlund-Nilsson and Nilsson 2000). Females directly benefit from choosing high-quality mates because males guard and care for eggs and young. Males in good condition fan their nests to circulate oxygen and also protect eggs from cannibalism by rivals. Males in poor condition eat eggs laid in their own nests (Candolin 2000).

Male throat coloration is arguably an "honest" signal, one in which the cost of expression varies with signal intensity. As such, signal intensity is a reliable indicator of the quality of a male as a potential mate or competitor (for a review of theoretical issues related to signal honesty see Kokko 1998) . Several factors help to maintain signal honesty. First, extreme color is correlated with lower parasite loads (e.g., Milinski and Bakker 1990, although see Candolin and Voigt 2001), Second, the pigments responsible for male throat coloration are either obtained from the environment (carotenoids; Brush and Reisman 1965; Simpson et al. 1981) or are physiologically expensive to synthesize (dropterins; Grether et al. 2001). Hence throat coloration likely correlates with foraging ability, metabolic efficiency, and/or the quality of (e.g., availability of nutrients in) the male's territory. Third, social interactions between rival males enact a fitness cost; false advertising draws attention from adversaries that might otherwise ignore the advertiser (Candolin 2000).

Detection depends on contrast between an object and its surroundings, so an optimal detector is maximally sensitive to such contrasts. An optimal identification mechanism is sensitive to features shared by all members of a class, e.g., conspecific males, and that distinguish those members from objects of other classes, e.g., heterospecific males. An optimal discrimination mechanism is sensitive to differences between individuals within the same class, such as differences in coloration between high and low quality conspecific males. The competing demands of discrimination and identification (and

potentially detection) should select for mechanisms that respond to different characteristics of relevant stimuli.

Selection acting on both signalers and receivers should lead to the evolution of identification mechanisms with minimal variance in response to the normal range of signal variation. In receivers, selection will favor identification mechanisms that unambiguously respond to signalers. In stickleback, identification mechanisms should have minimal sensitivity to individual differences in male throat color, while maintaining sensitivity to differences between throat colors and the colors of other types of objects in the environment. In signalers, a male with a throat color prone to misclassification will be at a selective disadvantage due to the relatively poor likelihood of being recognized by females as a potential mate. Consequently, selection should minimize variation in any aspect of male throat color that plays a role in species/sex recognition. This minimization can define an optimal identification mechanism.

In contrast to an identification mechanism, a discrimination mechanism should be maximally sensitive to variation among signalers. More specifically, selection should favor a discrimination mechanism that is maximally sensitive to signal characteristics that reliably indicate the signaler's quality, e.g., the extent to which the signaler can divert its resources to production of costly signals. Therefore, an optimal mechanism for discriminating stickleback throat colors can be defined as a mechanism that responds with maximal variance to the normal range of male stickleback throat colors or as one that responds with maximal variance to variation in the signal characteristics that most reliably indicate signaler quality.

Here we characterize male stickleback throat coloration and ask how spectral information should be processed by the stickleback visual system in order to optimally detect, identify, and discriminate conspecific males based on that coloration.

Materials and methods

Animal care

Fish of four gasterosteid species were collected from mid-March to early April by seining brackish-water pools and ditches near the eastern shore of Long Island, N.Y. The threespine stickleback, *G. aculeatus*, was the most common of the four species. The others were the blackspotted stickleback, *G. wheatlandi*, the fourspine stickleback, *Apeltes quadracus*, and the tenspine stickleback, *Pungitius pungitius*. Fish were collected shortly after *G. aculeatus* began arriving at the breeding grounds. Breeding individuals of at least two species were frequently collected in the same seine hauls, so breeding is sympatric at least on the scale of the pools.

Fish were transported to the laboratory and maintained under conditions simulating those of their breeding ground (6.0 ± 0.5°C; 8:16 h light:dark cycle; water made brackish by the addition of 12–18 g l^{-1} commercial sea salts) and fed frozen *Artemia salina* once daily. Male *G. aculeatus* expressing some development of coloration (blue iris, red mouth lining and/or throat) were slowly acclimated to conditions simulating their breeding habitat later in the spring

(22.0 ± 2° C; 16:8 h L:D cycle). Each animal was then isolated and maintained under continuous illumination provided by a single 25-W incandescent light suspended 20 cm above its 62-l (60×52×20 cm) tank. Each tank contained a sand-filled dish and filamentous algae (*Rhizoclonium* sp.) for nesting. Lighting was standardized so that interfish reflectance variation primarily resulted from inherent differences between fish rather than from any effects of illumination on the development of nuptial colors. After 2–3 days of exposure to simulated spring, fish established territories, constructed nests, and maximally developed nuptial coloration.

Microspectrophotometry

After a minimum of 8 h of dark adaptation, representative fish from each of the four species were euthanized by immersion in MS-222 and rapidly enucleated under dim red light. Photoreceptor isolation was performed under a dissecting scope equipped with infrared illuminators and image converters. Eyes were hemisected at the ora terminalis and retinas isolated from the posterior segment under phosphate buffered saline (pH 7.2) made hypertonic with 6% sucrose. Small pieces of retina were transferred to cover slips, cut and teased with fine needles and no. 11 scalpel blades in buffer, and sandwiched with another coverslip edged with silicone vacuum grease.

The computer-controlled, single-beam microspectrophotometer was described in Loew (1994). A 100-W tungsten-halogen lamp together with quartz/fluorite optics made it possible to carry out absorbance measurements from 330 to 750 nm using a 2 μm×5 μm measuring beam. Acceptable spectra (see Loew 1994) were smoothed with a digital filter routine ("smooft", Press et al. 1987) prior to normalization. The peak absorbance used for normalization was the maximum of the best fit Gaussian to data points 20 nm to either side of the estimated absorbance maximum of the alpha band. The wavelength of peak absorption (λ_{max}) of the smoothed, normalized visual pigment absorbance spectrum was obtained using the method of Mansfield as presented by MacNichol (1986). The templates used were those of Lipetz and Cronin (1988). Wavelength error of the MSP is ±1.0 nm; therefore, whole integer values of λ_{max} are reported.

Spectrometry: stickleback reflectance measurements

Reflectance measurements were performed on *G. aculeatus* males in breeding condition. Fish had been used previously in behavioral experiments and thus were somewhat adapted to handling. Animals were netted from their tanks and held with a damp towel or sponge. Fish were positioned against a plate with a small aperture to fix their position relative to the illumination sources and measurement optics. The entire measurement procedure generally took less than a minute from capture to release. Fish did not noticeably bleach during this time, though some stress-induced reflectance changes (particularly at UV wavelengths) cannot be ruled out.

Throat reflectance measurements were made from two different groups of fish, both acquired from the same location but during different years. In one data set, reflectances were measured with a CE395 Fast Spectral Scanner (Spectron Instrument; now Spectron Engineering, Denver, Colo., USA) from 2.5-mm² circular patches. With the CE395, two measurements were taken from each of 86 fish, one from the throat (between the opercula) and one from the flank. The CE395 was interfaced to a Gateway 2000 computer via a DASH 8 A/D board (Metrabyte; now Keithley Instruments, Cleveland, Ohio, USA). Radiance factors (C.I.E. 1977) were computed by comparing radiances from fish to those of an identically irradiated calibrated barium sulfate standard (Eastman Kodak Co., Rochester, N.Y., USA). The standard was assumed to diffusely reflect 99% of incident light. For these measurements, light was directed to the surface (fish or standard) at a 45° incidence angle, and light radiating along the surface normal was collected. The entire setup had a useable wavelength range of 395–725 nm.

Measurements of the second group of fish were obtained with an S2000 spectrometer (Ocean Optics, Dunedin, Fla., USA), a xenon arc lamp (Bausch & Lomb, Rochester, N.Y., USA), and a commercial reflectance standard (Whiteport; Ancal, Las Vegas, Nev., USA). In this data set, reflectances were measured from 3-mm² circular spots on fish maintained under conditions similar to those described above. All optical elements were removed from the arc lamp, and UV-visible lenses and fiber optic cables (Ocean Optics) guided light from the bulb to the fish and from the fish to the spectrometer. For these measurements, illumination was of normal incidence while reflected light was collected at 45° from normal. With this setup, 164 spectra were acquired from 33 fish on two different days. Generally three measurements, one directly between the opercula, one slightly rostral, and one slightly caudal, were made each day. This setup provided data at wavelengths ranging from roughly 320 to 920 nm.

Reflectance data were obtained from the irises of 9 additional fish held underwater and lightly anesthetized with 2-phenoxyethanol. These measurements were made with an S1000 spectrometer (Ocean Optics) over a wavelength range of 350 to 860 nm. A piece of Spectralon served as a standard.

Spectrometry: environmental light measurements

Measurements of environmental light were acquired with the S2000 on 10–12 April 1998. The timing coincided with the peak breeding period (W.J. Rowland, personal communication, 1998) for *G. aculeatus* in the tidal pools from which the fish were collected for reflectometry and MSP. During data acquisition, male threespine stickleback were seen building and defending nests. Females were seen less frequently, but several courtships and one spawning were observed. We measured irradiance with a cosine corrector (CC-UV; Ocean Optics) submerged inside a round-bottomed flask. We later determined that the cosine corrector significantly deviated from ideality at long wavelengths; the system was less sensitive than it should have been to off-axis light with wavelengths longer than 600 nm. Over the rest of the wavelength range, the instrument operated satisfactorily. Radiances were measured with a UV-visible collimating lens (36040; World Precision Instruments, Sarasota, Fla., USA) with a 4° acceptance angle. The lens was submerged inside a custom-built brass housing with a flat borosilicate glass window. The housing was painted black to minimize stray light. The spectrometer in both irradiance and radiance configurations was calibrated in the lab with a traceable tungsten filament light source (LS-1-CAL; Ocean Optics). For details of the calibrations, including quantification of the CC-UV's angular performance at long wavelengths see: http://www.psych.ucsb.edu/~rowe/calibration.html.

Various irradiance and radiance measurements were each acquired on two separate days. Data were obtained at different times of day and from several azimuthal directions so as to sample a variety of background areas and illuminations to which fish and surrounding substrate would be exposed. Optical axes of the sensors were directed horizontally; fish were assumed to view each other predominantly from the same depth (an assumption borne out by qualitative observations).

Computational modeling: general

We combined data from measurements of environmental lighting, fish reflectances, and photoreceptor spectral sensitivities to assess how fish might best detect, identify, and discriminate among male throat colors. In all computations, photoreceptor quantal catch rates were calculated as:

$$P = \int Q(\lambda)A(\lambda)d\lambda \tag{1}$$

where $Q(\lambda)$ is the quantal flux through the photoreceptor, and $A(\lambda)$ is its photopigment absorption spectrum. $A(\lambda)$ was computed using equations derived by Stavenga et al. (1993) so that optimal photopigments could be determined according to several different

criteria (see below) and compared to the pigments identified via MSP. When computing $A(\lambda)$, β-peak positions were set by an empirical formula from Palacios et al. (1998).

We generally computed quantal fluxes as:

$$Q(\lambda) = kR(\lambda)I(\lambda) \tag{2}$$

where $R(\lambda)$ is spectral reflectance of an object, and $I(\lambda)$ is the spectral irradiance illuminating that object. The constant, k, will be discussed under Results.

The fish used in this study breed in generally clear water and interact over short distances (generally less than a meter), so the effects of absorption and scatter by water were ignored. We also ignored absorption by pre-retinal media; to our knowledge no relevant data have been collected from any gasterosteid, but evidence from other fish suggests that the relevant transmissions through these animal's eyes are not strongly wavelength dependent (Douglas and Marshall 1999).

Cones rapidly adapt to maximize their responses to illumination changes that are small relative to the illumination's short-term temporal average (Normann and Werblin 1974), i.e., photoreceptors dynamically adjust their gains such that they are maximally sensitive to variation around the background radiance. To take such adaptation into consideration, we computed photoreceptor responses using an equation developed by Naka and Rushton (1966) and commonly used to model the responses of vertebrate photoreceptors (Shapley and Enroth-Cugell 1984):

$$E(\lambda_{\max}) = \frac{V}{V_{\max}} = \frac{P}{P + Ad} \tag{3}$$

where V is the difference between the photoreceptor's membrane potential and its potential in the dark, $V_{\max}$ is V when the photoreceptor is saturated by light, P is quantal catch rate (Eq. 1), and Ad is a factor that defines the photoreceptor's adaptation state at a given time. For each set of computations, Ad was set equal to the quantal catch rate of the photoreceptor when illuminated by the background radiance since this appropriately sets the photoreceptor's sensitivity.

Computational modeling: optimal photopigments

We computed the responses of photoreceptors to light from the average male throat so that we could identify photopigments optimized for throat detection. In our computations, a photoreceptor's response to light from the background is 0.5 (insert $P = Ad$ in Eq. 3). Consequently an optimal detector—one that on average best allows its bearer to notice a male stickleback throat in the breeding pool environment—would be one with responses maximally different from 0.5 when stimulated by light from male throats. We computed responses while varying photopigment $\lambda_{\max}$ to see how the MSP-determined stickleback photopigments compared against hypothetical pigments according to this criterion.

To test for optimality in discrimination, we computed responses of a photoreceptor to light reflected from each of the measured male throats and then computed the variance of those responses. All else being equal, a larger variance implies the photoreceptor will better allow its bearer to distinguish differences among male throat colors. We then varied $\lambda_{\max}$ to search for photopigments optimized for this task.

Computational modeling: optimal photopigment combinations

Animals process color by comparing the outputs of photoreceptors of different types (i.e., with different values of $\lambda_{\max}$). This comparison is performed generally (if not universally) with opponent processing—nervous systems subtract responses of photoreceptors with different spectral sensitivities. In the human visual system, there are two such information channels. In one channel, the output of middle-wavelength sensitive (MWS) cones is subtracted from the output of long-wavelength sensitive (LWS) cones, i.e., E(LWS)−E(MWS).

In the other channel, the output of short-wavelength sensitive (SWS) cones is subtracted from a sum of the outputs of MWS and LWS cones, i.e., [E(LWS) + E(MWS)]−E(SWS). A priori there is no reason to believe these particular opponencies are special. Even if an animal has a set of photoreceptors with spectral sensitivities similar to ours, it might not have a similar set of opponent processing mechanisms because of differences in the ecological problems faced by our respective ancestors.

The color hexagon (Chittka 1992) provides a graphical means to ask what color opponencies might be most useful to an animal performing a given task, and also to address the discriminability of colors in a generalized color opponent system. The hexagon is constructed from the responses of cones of three types. The response of a cone of a given type is represented as a vector whose length is proportional to that response (per Eq. 3, responses vary from zero to one) and whose direction is parallel to a line connecting the center of the hexagon and one of its corners. The vectors corresponding to the three different cone types are assigned directions that differ from each other by $\pm 120°$. The three vectors representing the responses of the three cone types to a given radiance (e.g., the light directed from a male stickleback throat to an animal's eye) are added from the center of the hexagon. The end point of the resultant vector is the representation of that radiance in the color hexagon. The background radiance to which the visual system is adapted (or any other radiance that equally stimulates all three cone types when adapted to this background) is located at the hexagon's center. A radiance that saturates one (or two) cone type(s) without stimulating the remaining cone type(s)—a practical impossibility given the broadband nature of the cone absorption spectra—would be represented at one of the hexagon's corners.

The hexagon representation has many interesting features. Of paramount importance for this study is that a given opponent color channel can be described by an axis passing through the hexagon (Chittka 1992). Therefore a given axis through color hexagon space describes an opponent color channel that could exist in an animal with a given set of photopigments. The direction of such a line through the hexagon indicates the weights given to the responses from each of the photoreceptor types providing inputs to the corresponding opponent channel.

As discussed below, stickleback have four cone pigments. We designate the pigments UVS (ultra-violet sensitive), SWS, MWS, and LWS. Because the color hexagon representation is based on the outputs of only three receptor types, these analyses were restricted to the use of three pigments at a time. As shown below, the SWS, MWS, and LWS cones are the receptors that provide the most useful information about male throat colors, so most of our analyses were restricted to combinations of the signals from those three cone types.

Maximum dispersion of throat colors in color hexagon space

We computed the spread of throat representations in the color hexagon because this statistic is relevant to the discriminability of throats in the absence of assumptions about specific color opponent mechanisms. To compute this dispersion we determined the mean position (centroid) of the throat representations in the hexagon, and then computed the mean Euclidean distance of all points from that mean position. Larger values of this statistic mean that the points comprising the population are, on average, farther away from each other. A larger spread implies more effective discrimination. We tested for optimality by computing geometrical spread as a function of $\lambda_{\max}$ for each individual pigment, given the spectral tuning of the other two pigments.

Linear distribution of throat colors parallel/perpendicular to primary axes of color space

Preliminary analyses suggested that in SWS/MWS/LWS color hexagons, throat colors are linearly distributed along an axis corresponding to an equally-weighted opponency between LWS

and SWS cones. As discussed below, such a distribution is potentially optimal because it implies the existence of a physiological representation of throat colors that facilitates discrimination of the relevant variation without compromising the utility of throat color as an aid in species recognition (identification) by an independent (orthogonal) opponent mechanism. We assessed the optimality of a photopigment combination by computing the slope of a linear fit through its hexagon representation of throat colors. For ease of interpretation, color hexagons were oriented such that E(LWS)-E(SWS) axes were horizontal and thus had zero slopes (as expressed in Cartesian coordinates). Therefore, we defined optimal photopigment combinations as those that represented the distribution of throat colors along zero-slope lines.

To see how well each photopigment was optimized given the other two, we computed the slope of the throat color distribution as a function of the λ_{max} of that pigment. We thus determined the sensitivity of this optimization to the spectral tuning of each pigment. In a separate analysis, we performed multi-dimensional searches among all possible photopigment absorption spectra. We used MATLAB's fmins function (The MathWorks, Natick, Mass., USA) to find photopigment combinations that represented male throat colors along a line with zero slope. By starting the search routine with different values for the three photopigment λ_{max}s, we found different photopigment combinations that satisfied this criterion equally well. We further evaluated these pigment combinations by computing the distance between the center of their hexagon and their representation of the average male throat. This distance is a measure of how well the pigments aid detection; the larger the distance, the more throat color representations differ from the background. We also compared optimal pigment sets by computing the overall spread of throat colors in their color hexagons, as well as that spread broken down into Cartesian components. Breaking the spread down into components allows us to address how efficiently the fish could identify and discriminate throat colors — a small spread along the putative identification (vertical) axis implies more reliable use of male stickleback throat color for identification, whereas a large spread along the discrimination (horizontal) axis implies a greater ability to discriminate among males based on differences in throat color (Fig. 1). Having identified pigment sets optimized for detection, identification, and discrimination, we then compared the actual stickleback pigments' capabilities against the capabilities of these optimal sets.

With inclusion of the UVS cones, there are four possible three-way comparisons of stickleback cone responses. For the S2000 data set we created color hexagon representations to examine all three-way comparisons. We sought linear distributions of throat colors in each of these color spaces. We quantified the extent to which throat color representations were linearly distributed by quantifying the residual variation, i.e., mean distance between individual throat color representations and the line fit through their distribution.

Computational modeling: optimal throat colors

In the analyses described above, we used the actual throat reflectances, and cone pigments were treated as variables subject to evolutionary change. In one additional analysis we approached the optimization from the other direction. Still assuming that throat colors would be optimally represented along a zero-slope line through an SWS/MWS/LWS hexagon with its MWS axis aligned vertically, we sought to determine how well optimized throat reflectances are if we assume reflectances can vary and cone pigments are fixed. We varied throat reflectances by shifting them along the wavelength axis. We shifted the entire throat reflectance data set and then determined the representations of these shifted reflectances in the SWS/MWS/LWS hexagon. By computing the slope of a line fit through the distribution of reflectances as a function of these artificial shifts, we determined the extent to which throat reflectances are optimized with respect to the cone pigments.
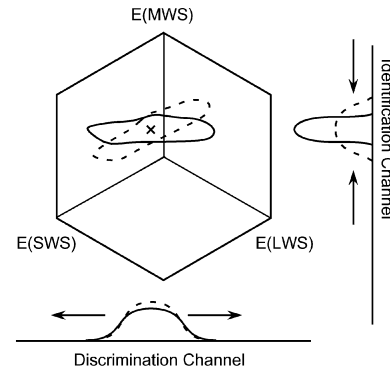
Fig. 1 Identification/discrimination model. If stickleback throat colors are distributed in color space as indicated by the region encompassed by the *solid curve*, two information channels are suggested: E(MWS)−[E(LWS)+E(SWS)]/2, and E(LWS)−E(SWS). The former channel can be used for effectively identifying stickleback throat colors, and the latter channel can be used for effectively discriminating throat colors. If throat colors are distributed as per the region encompassed by the broken line, the proposed identification and discrimination axes will not be as beneficial. Plots outside the hexagon indicate hypothetical distributions of responses in the two channels when presented with the corresponding distributions of throat colors. *Arrows* indicate directions that distributions should change for improved performance. The *x* marks the centroids of the throat color distributions, and the distances from the center of the hexagon to those centroids indicate how easily the average throat color can be detected against the background. *MWS* medium-wavelength-sensitive, *LWS* long-wavelength-sensitive, *SWS* short-wavelength-sensitive

Iris comparisons

In most populations, male stickleback nuptial coloration consists not only of the red throat, but also a large and conspicuous blue-green iris, so we addressed the possibility that male throat colors function to enhance iris color rather than to provide an independent metric of quality. Throat colors might accentuate iris colors by occupying the complementary region of color space, and thereby increasing the apparent saturation of the iris's color by means of a simultaneous contrast effect. To find the complement of the iris color, we extended a line from the average iris color representation in color hexagon space through the color neutral point to the color space's opposite edge. We then asked whether more extreme throat colors approach this complementary hue. We compared the location of the complementary hue to the point where an extension of the line fit through the distribution of throat colors reached the edge of color space. Lastly, we shifted throat reflectances along the wavelength axis to ask how far the reflectances need to be shifted in order to bring the extension of the throat color distribution into register with the iris color's complement.

Results

Microspectrophotometry

As noted above, females of all four stickleback species (*G. aculeatus*, *n* = 6; *G. wheatlandi*, *n* = 6; *A. quadracus*, *n* = 5; *P. pungitius*, *n* = 5) were found to have four visual pigments. The pigments could be fit with vitamin A_2 nomograms, although some of the intra-fish variation suggested a mixture of A_1 and A_2 pigments. The λ_{max}s of photopigments in all four species were around 360 nm

(UVS; range 360–365 nm) and 445 nm (SWS; range 440–450 nm) for two classes of single cone, and 530 nm (MWS; range 519–535 nm) and 605 nm (LWS; range 575–625 nm) for the two halves of the double cones. These results are similar to those of a prior report (Lythgoe 1979), except that UVS cones were not characterized in the earlier study. All four species examined here had a typical teleost square mosaic (Ali and Anctil 1976) with the SWS and UVS cones presumably filling the squares' centers and corners, respectively. The unusually large range of λ_{max} values for the LWS pigments suggests the possibility of polymorphism.

Spectrometry: stickleback reflectance measurements

All throat reflectance measurements exhibited a peak at roughly 630 nm. Figure 2a, c shows summaries of data collected with the CE395 and S2000 respectively. Figure 2b, d demonstrate the somewhat counterintuitive finding that most of the variation in throat color is at the short-wave end of the spectrum (400–550 nm), i.e., variation in "redness" is not due to variations in reflectance at the "red" end of the spectrum. This result is consistent with the well-established fact that stickleback throat redness arises primarily from the deposition of carotenoids (e.g., Wedekind et al. 1998) that provide color by selectively absorbing wavelengths at the short-wave end of the human-visible spectrum (drosopterins, if present, similarly absorb short wavelengths; Grether et al. 2001).

In addition to the 630-nm peak, the data acquired with the S2000 frequently showed one or two minor UV peaks. Figure 2e shows sample traces of these data. Compared to the CE395 data over their common range, the absolute reflectances in the S2000 data were lower and shifted by 5–10 nm toward shorter wavelengths. These discrepancies were probably due to differences in the equipment. Theoretically, the methods should have produced identical results, but differences in acceptance angles of the lenses, the accuracies of the calibrations of the two instruments, and other such optical factors would produce discrepancies. However, the differences could have resulted from intrinsic reflectance differences between the two groups of fish. Intrinsic differences might have resulted from differences in housing conditions, phases of the reproductive cycle during which measurements were made, or the overall health of the fish. In any case, as we will show, the modeling results reported below are not appreciably affected by the differences between these two data sets, so we believe that the conclusions we present are robust.

Several spectra (not shown) obtained with the S2000 had gentle slopes with little or no inflection between 400 and 600 nm. Some of the 22 fish measured on separate days were characterized by such spectra in measurements made during one session but not the other. Similarly, UV peaks were more or less prominent in individual fish compared across days. In assessing male
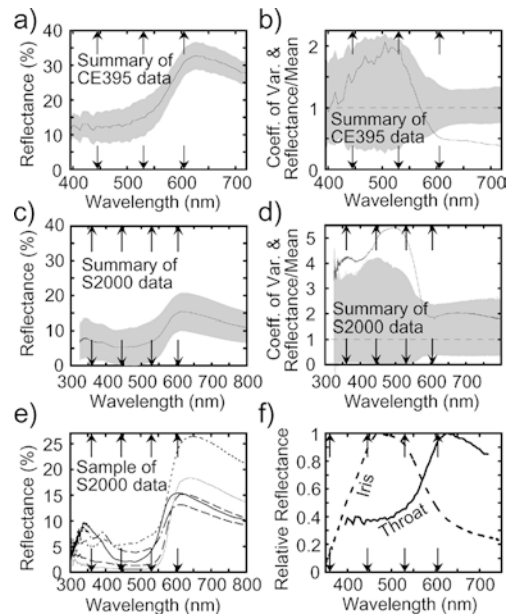
Fig 2a–f Variation in male *G. aculeatus* reflectance. Most of throat reflectance variation is in the short- and middle-wavelength regions of the spectrum. *Solid lines* in **a** and **c** show mean reflectances of throats. *Shaded regions* encompass ± 1 SD around that mean. *Solid lines* in **b** and **d** depict coefficient of variation (variance/mean). *Shaded regions* provide an alternative depiction of variation in the data: each spectrum was divided by the mean of all spectra acquired with the same instrument; the extremes of the curves resulting from this computation were bounded by the borders of the shaded area. Were there no variation, coefficients of variation would be zero and shaded regions would be restricted to the *dashed lines*. Each curve in **e** depicts data from a single measurement acquired with the S2000. These curves exemplify variation in the UV region of the spectrum and its effective independence from variation at the long-wave end of the spectrum (note that these spectra represent a small sample of the data collected with the S2000). The plots are depicted with different dashing schemes only to aid in distinguishing them. In **f** the solid line is the mean reflectance as per **a**, but the data have been normalized. The *dashed line* is the mean normalized reflectance from the irises of nine fish. In all panels, the *arrows* indicate the positions of the MSP-determined λ_{max}s of stickleback visual pigments

quality, inter-fish variation is of prime concern. In asking how the animals visually process color, however, we need only consider the distribution of possible throat colors. On the basis of behavioral findings (Rowland 1994), we assume that higher quality males will generally have more extreme coloration expressed over a larger area of their bodies. However, the color of individual males can change on short time scales (e.g., through the activity of melanophores). It is beyond the scope of this paper to quantify variation in reflectance within individual fish over time and anatomical location. We therefore treated all measurements as equivalent; rather than, for example, averaging all of the measurements from the same fish, we treated each measurement as a throat reflectance spectrum that might be presented to a potential mate or rival.

The small number of irises sampled yielded extremely variable results in terms of absolute reflectance, but the spectral pattern was consistent. There was always one
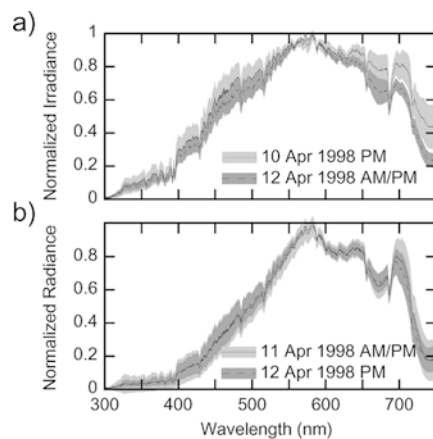
peak, and in eight of nine measurements that peak was located between 460 and 500 nm. As shown in Figure 2f, iris reflectance is essentially the inverse of throat reflectance. Iris reflectance is high where throat reflectance is low and vice versa.

Spectrometry: environmental light measurements

Absolute quantal fluxes varied by just slightly under two orders of magnitude for both radiance (background) and irradiance (illumination) measurements. However, the shapes of the spectra were consistent across time of day and look angle (Fig. 3). The main exception to this generalization occurs in the irradiance data at wavelengths longer than 600 nm. This long-wave discrepancy is likely due to the instrumental artifact described above, although it might also result from slight differences in the photosynthetic state of the flora in the water from one day to the next. Irrespective of cause, even these discrepancies are relatively minor. The mean normalized irradiance spectra acquired on the two different days agree to within 20% for essentially all wavelengths shorter than 700 nm.

Cryptic coloration of male flanks

No direct measurements of substrate reflectance were made, but substrate reflectance could be approximated using radiance and irradiance data. Since the variances of normalized radiance and irradiance were small, dividing the former by the latter provides a reasonable estimate of the substrate's average relative spectral reflectance. The computation is not strictly correct because the measurements of radiance don't correspond to measurements of irradiance of the same point in time and space, but the narrow ranges in radiance and irradiance suggest that any true measurement of the average substrate reflectance would be similar to the estimate obtained this way.

In Fig. 4a, we compare this normalized substrate reflectance estimate to the mean normalized reflectances of stickleback throats and flanks. Note that the estimated substrate reflectance closely matches the measured reflectances of male stickleback flanks. Qualitative observations of fish in the field indicate that the match is not just relative—when motionless, *G. aculeatus* are exceedingly difficult to detect from above (noted for another population by Blouw and Hagen 1990). Therefore, the absolute reflectance of the background must be the same as that of the fish flank (Fig. 4b). We used the scale factor converting the background estimate from relative reflectance to absolute reflectance to derive an appropriate value for the constant, k, in Eq. 2. Note that Fig. 4b also shows the absolute reflectance of the average male throat relative to that of the flank (measured) and substrate (estimated).

Computational modeling: optimal photopigments

Figure 5 depicts the results of computations designed to find photopigments optimized for detecting (Fig. 5a) and discriminating (Fig. 5b) male throats. These computations were carried out using three different sets of assumptions. The solid curves were derived from throat reflectance data acquired with the CE395; the dashed
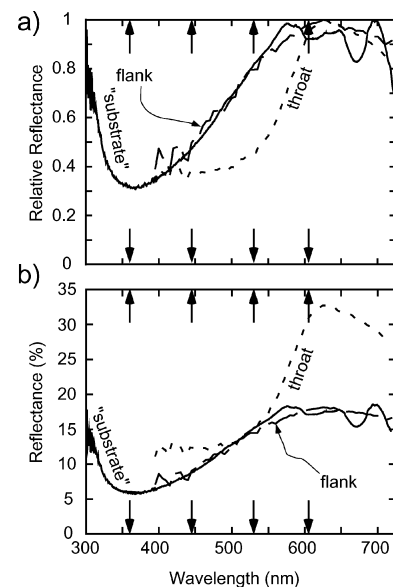
Fig. 4a,b Reflectance comparisons. *Solid curve* in **a** is estimated reflectance of the substrate at a time and location where fish build and defend nests. The *dotted line* is the same mean throat reflectance data shown in Fig 2f. *Dashed curve* shows mean reflectance from flank region of fish measured and computed exactly as data from throats. In **b** data are represented in absolute terms. Scaling of substrate data performed as described in text
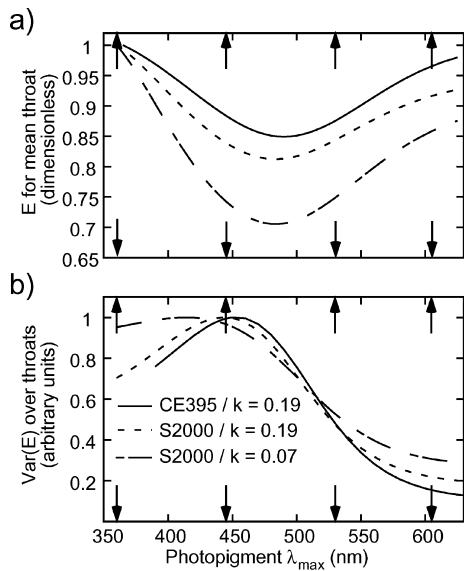

Fig. 3a,b Environmental lighting in a stickleback breeding pool. Plots in **a** depict the irradiance (illumination) spectra. Plots in **b** depict radiance spectra (essentially the light emanating from small patches of background). All plots were normalized in quantal flux units. **Lines** indicate means and **shaded regions** 1 SD around those means for all spectra acquired on a given day as indicated by the inset legends. *AM/PM* means measurements made both morning and afternoon

Fig. 5a,b Optimization of throat color detection and discrimination by a single photopigment. In **a** mean responses to a set of fish throats are plotted against λ_{max}. In **b** variance in photoreceptor outputs are computed as a function of photopigment λ_{max}. To generate these curves: for each photopigment λ_{max}, photoreceptor outputs were computed for cones viewing light reflected from a set of fish throats. *Solid curves* were derived from reflectances of the 86 fish measured with the CE395. *Dashed curves* were derived from measurements of 33 fish with the S2000. For the *solid* and *single-dashed curves*, the value of k (Eq. 2) was set to minimize the difference in mean flank reflectance and computed substrate reflectance as described in the discussion surrounding Fig. 4b. Values for the *double-dashed curve* were computed with a lower value of k potentially more appropriate for the S2000 data set. Results have been normalized. *Arrows* indicate the λ_{max}s of the actual gasterosteid pigments

curves were derived from data acquired with the S2000. In all cases shown, the throats were assumed to be illuminated by light with a spectrum equivalent to the mean irradiance spectrum measured in the field and the photoreceptors were assumed to be adapted to the mean radiance spectrum measured in the field. The two sets of computations on the S2000 data (dashed curves) were performed using different values of k (Eq. 2) as indicated in the figure legend. In one case, the value of k was selected to provide an absolute match between fish flank and background ($k = 0.19$; see Fig. 4b). In the other case, k was rescaled under the additional assumption that differences between the CE395 and S2000 reflectance measurements (Fig. 2) were artifactual, and that the CE395 overestimated the throat and flank reflectances (or equivalently, that the S2000 underestimated throat reflectances). All three of the analyses in Fig. 5a suggest that pigments with extremely long or short wavelength λ_{max}s will provide larger signals for detection of male throat color against the average tide pool background than would pigments with intermediate λ_{max}s. Figure 5b shows the variance in the response of a photoreceptor when viewing the range of measured throat colors. All curves contain a single peak located near the λ_{max} of the SWS pigment. Results similar to those in Fig. 5 were

also obtained assuming spectrally flat illumination and adaptation spectra (not shown).

Some of the differences between the solid and dashed curves in Fig. 5 could conceivably be attributed to the UV light measured by the S2000 but not the CE395. Overall, however, the similarity of the curves indicates that the presence or absence of UV reflectance and other differences in the reflectance spectra obtained by the two instruments (see above) do not appreciably affect the conclusions of this analysis. We also analyzed the data from the S2000 exclusive of the UV portion of the spectrum (in an effort to make the two data sets more nearly equivalent methodologically) and again found similar results.

Computational modeling: optimal photopigment combinations

Unless otherwise stated, parameters (i.e., data set, value for k) used in the analyses reported in the remainder of this paper are the same as the parameters used to generate the solid curves of Fig. 5. In Fig. 6, responses to flank and throat reflectances are shown in an SWS/MWS/LWS color hexagon. Responses to the flank encompass the neutral point at the hexagon's center as should be expected by the match between substrate and flank reflectances (the flank spectrum of one fish had to be discarded due to an error during data recording). Throat and flank responses overlap to some extent, though throat responses are generally displaced toward the bottom of the color hexagon.

As noted in Materials and methods, the color hexagon representations of throat colors cluster along a line roughly parallel to an E(LWS)-E(SWS) axis (Fig. 6). Therefore, a discrimination axis created by subtracting equally weighted outputs of SWS and LWS receptors would be sensitive to a large proportion of the variation in male throat color. The linear distribution of throat colors is also essentially perpendicular to an E(MWS) axis. An E(MWS) axis in this color space is coded by neurons that average the responses of SWS and LWS cones and subtract that average from the response of MWS cones. Such neurons would be largely insensitive to throat color variation and thus would be well suited to function as part of an identification channel.

A similar distribution of throat color representations was obtained with the S2000 data, so we conclude that variation in UV reflectance (or lack thereof) has little to no bearing on this analysis. We directly address this point again below when we include analyses with UVS cones.

Maximum dispersion of throat colors in color hexagon space

The analyses presented in Fig. 7a provide assessments of the optimality of the combination of stickleback SWS,

a)

b)
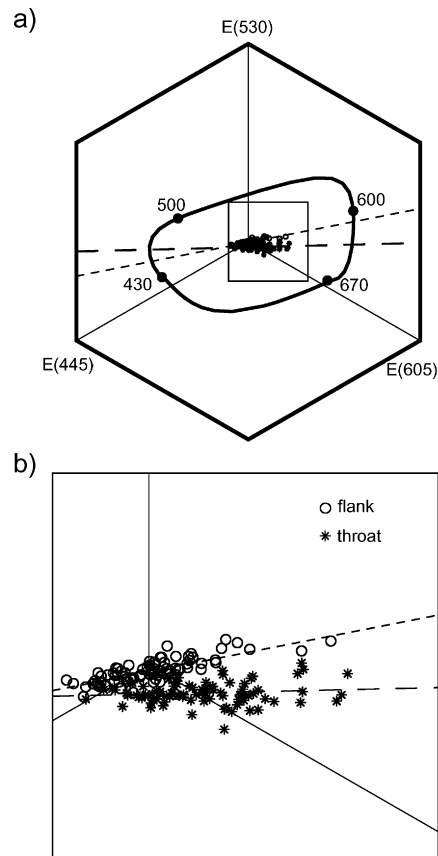
Fig. 6a,b Variations in color space. *Asterisks* represent the responses to male throats illuminated by environmental irradiance (Fig. 3a) when receptors are adapted to environmental radiance (Fig. 3b). *Open circles* represent the responses to flanks under the same conditions. The *long and short dashed lines* represent linear fits to the throat and flank distributions, respectively. *Solid curve* depicts the locus for spectral lights having the same quantal flux as the adaptation spectrum. In **a** the wavelengths of four of those spectral lights are indicated; the segment joining the lights at 430 nm and 670 nm was constructed from various ratios of a mixture of those two spectral lights. The *gray dot* in the center where the three hairlines intersect marks the color neutral point. In **b** the *area inside the square* in **a** is shown at higher magnification

MWS, and LWS visual pigments for absolute discrimination of throat colors. Each curve shows the overall dispersion of throat colors in color space as a function of the λ_{max} of one pigment when the other two pigments are fixed. Given the MWS and LWS pigments, the SWS pigment is optimally positioned to maximize discriminability according to this metric. In contrast, the tuning of the MWS pigment has the opposite effect, i.e., to minimize throat color discriminability. The LWS pigment would provide for better throat color discrimination if it were shifted toward longer wavelengths.

## Linear distribution of throat colors orthogonal to one of the primary axes of color space

As outlined in Materials and methods and detailed in the Discussion, an optimal design for the coding mecha-

a)

b)
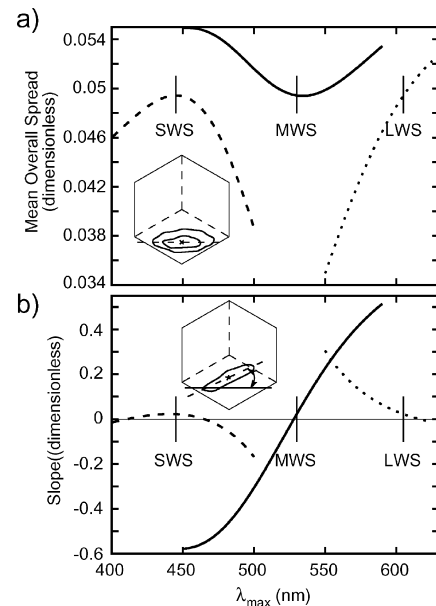
Fig. 7a,b Optimizing discriminability. *Curves* in **a** represent mean distance of throat colors from centroid of their distribution in color hexagon space as indicated by inset. *Dashed line* represents spread as a function of λ_{max} of the SWS cone while MWS and LWS cones are held fixed. *Solid and dotted curves* indicate spreads when only MWS and LWS pigments, respectively, are varied. *Vertical lines* indicate measured photopigment λ_{max}s. In **b** the ordinate is slope of line fit through the representations of male throats in color hexagon space as indicated by the angle depicted in the *inset*. *Dash pattern* conventions as in **a**

nisms that identify and discriminate male throat colors produces a linear distribution of throat color representations orthogonal to one of the photopigment axes in color hexagon space. For ease of interpretation, we oriented the appropriate axis—the MWS axis—vertically, so an optimum photopigment combination is one that represents the distribution of throat colors along a horizontal axis and thus has a slope of zero in Cartesian coordinates (Fig. 6). In Fig. 7b we show how the slope of a line fit through the color hexagon representation of throat colors depends upon the λ_{max} of each pigment. In this analysis, the SWS pigment's λ_{max} is essentially irrelevant as long as it is less than around 470 nm. On the other hand, the slope strongly depends upon the λ_{max} of the MWS pigment. The MWS pigment must have a λ_{max} near its optimum around 528 nm; if the λ_{max} was at a longer or shorter wavelength, the distribution of throat colors would exhibit a positive or negative slope respectively, with a corresponding loss of coding efficiency (Fig. 1). The λ_{max} of the LWS pigment is also constrained but only from one direction. The slope will be close to zero as long as the LWS λ_{max} is larger than around 600 nm. Given the spectral position of any two pigments, the third is positioned nearly optimally (LWS and MWS) or within a broad region where the exact value is inconsequential (SWS) according to this analysis.

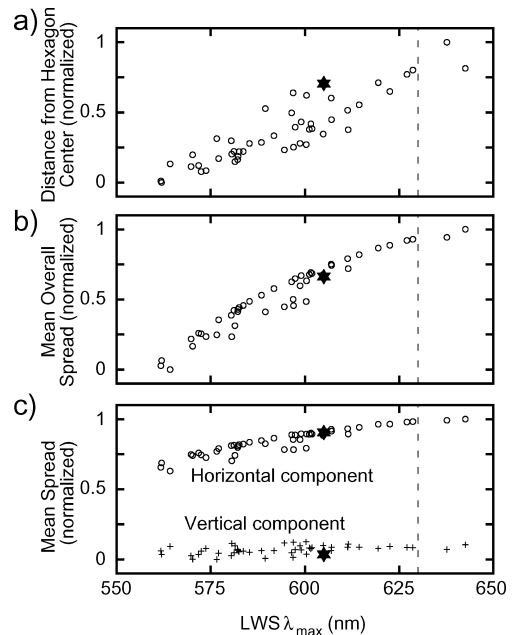Multi-dimensional searches of photopigment space found many photopigment combinations that distrib-
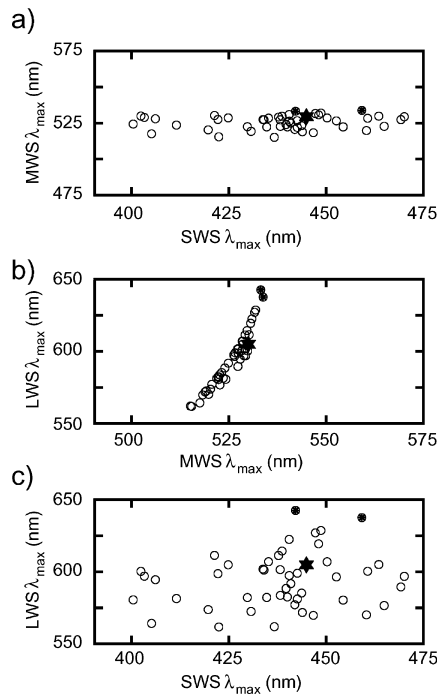
Fig. 8a–c Optimal pigments. The space of all possible pigments was sampled to find triplet combinations that have responses to male throats spread out along an E(LWS)-E(SWS) axis. *Filled hexagrams* represent the MSP-determined photopigment triplet that we found in threespine stickleback. *Points with asterisks* in their centers are unlikely to be produced because the LWS pigment's λ_{max} is beyond the range for photopigments that have been identified in any animal. For an alternative depiction of these data, see http://www.psych.ucsb.edu/~rowe/OptPigs.html

Fig. 9a–c How to build a better fish. Each point corresponds to the results of computations using one of the triplets from Fig. 8. In **a** distance from the color neutral point to the centroid of throat color distribution (a measure of detection) is shown as a function of the LWS pigment's λ_{max}. In **b** mean distances of male throat representations from the centroids of their distributions—the same statistic (a measure of discrimination) as that computed for Fig. 7a—are depicted. In **c** the distance from the centroid is broken down into components along the horizontal [E(LWS)-E(SWS)—*open circles*; another measure of discrimination] and vertical [E(MWS)−(E(LWS)+E(SWS))/2—*crosses*; a measure of identification] axes. In all panels the *filled hexagram* represents results using the actual color triple (SWS = 445; MWS = 530; LWS = 605) determined via MSP

uted throat colors along a line with zero slope. Beginning the searches from 50 different combinations, we identified 46 unique optima and characterized the essential features these optimal combinations share. Those features are the absolute λ_{max} of the MWS pigment (always between about 515 and 535 nm; Fig. 8a, b), and the ratio between LWS and MWS λ_{max} (Fig. 8b). Consistent with our previous result (Fig. 7b) the λ_{max} of the SWS pigment appears to be largely irrelevant in this optimization (Fig. 8a, c), whereas the MWS pigment's λ_{max} is tightly constrained (Fig. 8a, b).

In Fig. 9 we show the results of analyses of the 46 photopigment combinations with respect to other forms of optimization. The detectability of the average male throat (Fig. 9a) and the absolute discriminability of throat colors (i.e., their overall spread in the color hexagon; Fig. 9b) are positively correlated with the λ_{max} of the LWS pigments of these combinations. Results shown in Fig. 9c demonstrate that all of the photopigment combinations are roughly equivalent with respect to optimization of identification, but discrimination along the E(LWS)-E(SWS) axis is positively correlated with LWS λ_{max}, just as is the absolute discriminability (Fig. 9b).

In Fig. 10 we represent the data acquired with the S2000 in hexagons using all possible combinations of

stickleback cone types. With these data, which include UV wavelengths, the slope of the line in the SWS/MWS/LWS representation is somewhat larger than with the CE395 data, but still indistinguishable from zero (slope ± 95% confidence interval = 0.067 ± 0.10). Other cone response combinations do not spread the throat colors out along any line as well as does the SWS/MWS/LWS combination. The mean distances from data points to the best-fit lines are 0.010 (SWS/MWS/LWS), 0.032 (UVS/SWS/MWS), 0.020 (UVS/MWS/LWS), and 0.036 (UVS/SWS/LWS); smaller values indicate closer fit to the lines. The closer the representations of male throat colors approximate a linear distribution, the more efficiently color opponent axes perpendicular to and parallel to these two axes can be used identify and discriminate those colors.

Computational modeling: optimal throat colors

If we reverse our approach and ask if throat reflectances are optimized to the stickleback photopigment spectral sensitivities, we find that throat reflectances are optimized to within 2 nm, i.e., shifting throat reflectances
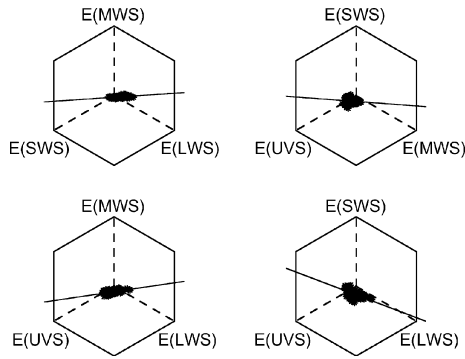
Fig. 10 All pigment combinations. Color hexagons constructed as in Fig. 6, but with the S2000 data set and all possible variations of the four MSP-determined cone types. *Solid lines* indicate best fits through the data. *Dashed lines* intersect at the color neutral point in each hexagon

2 nm along the wavelength axis causes the throats to be represented precisely orthogonal to the E(MWS) axis in the SWS/MWS/LWS color hexagon.

Iris comparisons

In Fig. 11 representations of iris colors are plotted in an SWS/MWS/LWS color hexagon. Iris color representations are close to an extension of the axis along which throat colors are represented. Moreover, a line extended from the mean iris color through the color neutral point passes close to the most extreme throat color, indicating that iris and throat colors are complementary. Male throat coloration may thus enhance the conspicuousness and, consequently, detectability of the iris and vice versa. On the spectrum locus, the light that complements the mean iris color—the point where a line passing through the mean iris color and the color neutral point
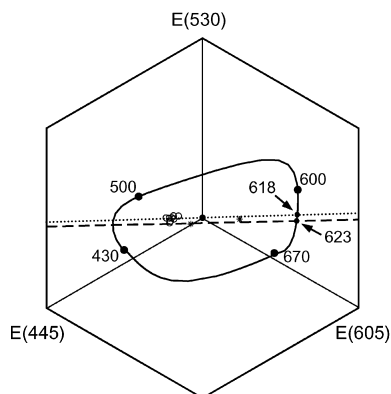
Fig. 11 The relative representations of iris and throat colors. *Long-dashed line* indicates a linear fit through the points generated from actual stickleback throat reflectances (from Fig. 6). *Asterisks* mark the data points with the most extreme horizontal positions in color hexagon space representations of those reflectances. *Solid curve* is spectrum locus (as in Fig. 6). *Open circles* indicate representations of eight iris reflectances as would be seen by stickleback in the breeding environment. *Dotted line* connects mean iris color and color neutral point

intersects the spectrum locus—has a wavelength of 618 nm, while the line fit through the throat representations intersects the spectrum locus at 623 nm. A shift of the throat reflectances by approximately 5 nm toward shorter wavelengths causes the intersection of these two lines with the spectrum locus to coincide exactly.

Discussion

General

Adaptive explanations for features of color vision are easy to propose but difficult to verify (Chittka and Briscoe 2001). One of the most studied signal/receiver systems in this regard is the color vision of insect pollinators and the flowers with which they interact (Chittka 1996, 1997; Chittka and Briscoe 2001). Initial studies (e.g., Chittka and Menzel 1992) were generally interpreted to indicate that hymenopteran visual pigments are optimized for representing floral colors (despite the authors' disavowal of this interpretation; Chittka and Briscoe 2001). It is more likely that hymenopteran visual pigments evolved to their present states before flowers evolved (Chittka 1997), suggesting instead that flower colors evolved to "exploit" the sensory biases in the visual systems of ancestral insects. Similarly, although we have presented data indicating that stickleback photopigments have spectral sensitivities optimized for representing stickleback nuptial colors, parsimony suggests the visual pigment sensitivities evolved first. It appears that all four gasterosteid species in our study have the same cone pigments. However, only *G. aculeatus* signals with reddish throat colors.

The evolutionary history we are trying to untangle is potentially paralleled not only by insects and flowers. Similar scenarios may be proposed, for instance, for primates and fruit; did trichromacy evolve in primates to aid in detecting and selecting ripened fruit (Hunt et al. 1998; Mollon 1989; Osorio and Vorobyev 1996; Regan et al. 1998; Smith et al. 2003), or did fruit color evolve to attract seed dispersers more effectively? Our proposal that the relevant component of variation in throat color should be represented along a line through color space may provide useful insight into many such similar questions concerning the evolution of signals and receivers. Indeed, a linear representation of bowerbird feather colors in bird color space has already been discovered (J.A. Endler, personal communication, 2001), so this pattern of variation in the hypothesized perceptual space of the receiver is not restricted to fish. We will return below to specific questions about the order of evolutionary events in stickleback.

Linear distributions and the processing of color information

The overall dispersion of signal colors in an animal's color space provides a measure of discriminability that does not take into account constraints imposed by other

visual tasks such as identification. In addition, overall dispersion is not directly applicable to the question of how coloration can be translated into a specific metric of quality (e.g., how throat color relates to carotenoid concentration and hence overall condition). Measures of overall dispersion may be significant in the context of individual recognition but are unlikely to provide insight into the design of signals or receivers in the contexts of species recognition and adaptive mate choice.

For evaluation of signaler quality, variation along one axis in color space may be critically important (e.g., variation resulting from differences in pigment concentration that reflect male fighting ability, foraging efficiency), while variation perpendicular to that axis may contain little or no information that has fitness consequences for the receiver. Consequently, selection should favor (1) high quality signalers that exhibit more extreme values of color along the axis in color space that provides the most reliable indicator of signaler quality, and (2) increased sensitivity to this variation by the assessment mechanisms of receivers. At the same time, variation perpendicular to the primary axis of color variation may be selected against if it is unrelated to signaler quality and/or the response of an orthogonal processing mechanism is used to determine the signaler's sex and/or species identity. The conflicting demands of identification and discrimination, therefore, may select for a linear distribution of colors in the receiver's color space.

We know of no data addressing the question of what opponent channels stickleback use to encode color information. However, independent of our data and models, we can argue that the animals should have channels that are orthogonal in color hexagon space and comprised of pairwise comparisons of photoreceptor outputs with equal weighting. Equal weighting is sensible based on developmental rules. To build a nervous system with particular opponent channels requires that the system be able to calibrate those channels. Opponent channels comprised of neurons that equally weight the output of two cone types are easily calibrated using the spontaneous activity-dependent mechanisms known to operate on developing nervous systems (see section 3.2 of Sernagor et al. 2001 for a review of activity-dependent neural development). Calibration may be achieved by establishing oppositely signed inputs from the two cone types and adjusting their relative weights until there is no response when the two cone types are simultaneously activated by the waves of spontaneous activity that sweep across the retina during development (a neural analog of a Wheatstone bridge). In a survey of the opponent channels that likely encode colors in the visual systems of hymenopteran insects, Chittka et al. (1992) found that most species should have one opponent channel that compares the responses of a pair of receptor types weighted approximately equally, and another opponent channel that compares the average output of those two receptor types with the output of the third. We suspect that such channels are typical.

Cryptic flank coloration

An object will appear cryptic to humans as long as light from the object and light from its background produce similar responses in our three types of cone, even if the spectra of light from object and background are quite different. Encryption, like beauty, can reside in the eye of the beholder. An animal that appears cryptic to one species may not be cryptic to another species with different visual pigments and/or processing mechanisms (Heiling et al. 2003). Here we have provided evidence that flanks of males in our *G. aculeatus* study population are cryptic to any animal attempting to view them in their breeding pools (Fig. 4).

The preceding claim depends upon a quantitative match between reflectances of stickleback flank and tidepool substrate. This match, in turn, depends upon a scaling factor we can interpret as k in Eq. 2. In our modeling, we chose k by assuming flanks and substrates matched. As noted above, this assumption renders consistent our measurements of stickleback flank reflectance, our estimate of relative substrate reflectance, and the observation that males in their breeding environment are extremely difficult to detect from above (Fig. 4b, see earlier discussion). During the course of our computations, we manipulated various parameters and analyzed several variables not discussed here. One coincidence we discovered merits special notice. The value of k that minimizes detectability of flanks maximizes the discriminability of throats. That is, the variance in stickleback cone (particularly SWS cone) responses to male throat colors is maximal for that same value of k, as if the magnitude of throat reflectance has been optimized to make throat colors most discriminable to other stickleback when viewed against the average substrate.

Tuning of spectral sensitivities

Because researchers have generally rated stickleback throats in terms of "redness", one might presume throat color variation is primarily at the long wavelength ("red") end of the spectrum. Our measurements show this not to be so; the relative variation is largest at wavelengths shorter than 500 nm. Consequently, we conclude—independent of any modeling—that enhanced sensitivity of female stickleback to long wavelength light (Cronly-Dillon and Sharma 1968) will not help female fish discriminate among male throat colors. Indeed, our sample of throat colors produces greater variation in the responses of SWS cones than of either MWS or LWS cones.

Since the LWS pigment is relatively insensitive to throat color variation, (Fig. 5b) it is not particularly useful for discriminating among such colors. However, relative to other possible cones, the LWS cones have large responses to the average stickleback throat (Fig. 5a) suggesting that cones containing this pigment are good throat detectors. Thus, enhanced relative long

wavelength sensitivity of breeding-conditioned female *G. aculeatus* in comparison to other stickleback species (Baube 1994), and in comparison to themselves at other times of the year (Cronly-Dillon and Sharma 1968) might improve detection of conspecific males as "brighter" targets, even if it does not improve discrimination.

In contrast to the LWS cones, the SWS cones seem optimal for discriminating throat colors. This conclusion is supported by analyses either of individual cone responses (Fig. 5b) or of opponent combinations of cone responses (Fig. 7a). A combination of the optimally variable SWS cone output and relatively stable LWS cone output (Fig. 5b) may facilitate the animals' ability to discriminate among males using an E(LWS)-E(SWS) mechanism. Using the LWS cone responses as a reference would make the stickleback's judgement of "redness" largely insensitive to variation in the overall level of illumination.

Analyses presented in Fig. 7 indicate that selection has maximized variation of male throats along an E(LWS)-E(SWS) axis (Fig. 7b), rather than over the entire color space (Fig. 7a). The tuning of the MWS pigment would *minimize* the absolute discriminability of throat colors (Fig. 7a). Since throat color appears to be an honest signal of male quality, this minimization makes no sense unless it is offset by some larger benefit. We propose that this benefit is the coding efficiency of the simple identification/discrimination scheme outlined above. In this scheme, the discrimination mechanism does not receive input from the MWS pigment and so would be unaffected by a change in its spectral sensitivity. However, varying the position of the MWS pigment's λ_{max} has a profound effect on the sensitivity of the proposed identification mechanism to variation in throat color (Fig. 7b). The λ_{max} of the MWS pigment is remarkably close to the value that minimizes the proposed identification channel's sensitivity to throat color variation and, thus, makes the combination of the channel and throat reflectances useful for species recognition.

We can illustrate the importance of the MWS pigment's tuning by modeling the effects of a shift in its λ_{max}. Increasing the MWS pigment's λ_{max} by 10 nm produces a 14% increase in throat color spread along the identification axis. Although correctly identified throat colors will be just as discriminable (the proposed discrimination axis receives no MWS cone input), misclassifications would be more likely. The viewing animal would either have to relax its criterion for identification and thereby increase its false alarm rate, or it would miss conspecifics with signals outside the identification channel's criterion range. Furthermore, the responses of the identification and discrimination channels to throat color variation would no longer be independent; missed animals would likely be those with extreme coloration, including males signaling the highest quality.

To remove the correlation between the two channels, the fish's nervous system would have to use different weightings in its opponent channels. A 10-nm shift in the MWS pigment would require the animals to identify throat colors along a 0.99E(MWS)−0.39E(SWS)−0.6E(LWS) axis and discriminate them along a 0.13E(MWS)−0.93E(SWS)+0.8E(LWS) axis. While nothing theoretically precludes the photoreceptor's outputs from being processed with such weightings, it is not clear how such a system would develop. A system with equal weightings would be much simpler to calibrate (as described above), and thus would be a more likely mechanism to evolve in response to selection for coding efficiency.

The 445/530/605-nm pigment combination optimally distributes throat colors along an E(LWS)-E(SWS) axis through the color hexagon (Fig. 7b), but a multidimensional search shows that this pigment set is not unique in that regard (Fig. 8). Furthermore, other pigment sets equally optimal by that criterion might be superior by other criteria. As just described, the MWS pigment's λ_{max} is tightly constrained in the context of the 445-nm and 605-nm pigments. However, a 6- to 7-nm shift of the MWS pigment accompanied by a 25- to 40-nm shift of the LWS pigment would allow male throats to be more easily detected and discriminated without affecting their ability to be identified (Figs. 8, 9). On the other hand, the improvement is small (potentially invisible to selection; Chittka and Briscoe 2001), and probably subject to physical constraints—no animals are known to have pigments with λ_{max}s longer than about 630 nm (Lythgoe and Partridge 1989). Given these considerations and the involvement of the visual system in many other aspects of stickleback behavior (e.g., foraging, predator avoidance), the proximity of the current photopigments to a more globally defined optimum not only for throat color identification and discrimination, but also detection (Fig. 9a), is remarkable.

The anti-iris hypothesis

In addition to the identification/discrimination hypothesis, our data suggest another, not necessarily exclusive hypothesis: throat colors maximize iris conspicuousness in stickleback color space. We will refer to the second hypothesis as the anti-iris hypothesis. We postulate that extreme throat color may have evolved not as a signal in itself but to enhance the signal quality of the iris by forming a contrasting background. Iris representations are almost directly opposite the color neutral point from the most extreme throat colors and close to an extrapolation of the best-fit line through throat color representations (Fig. 11). This suggests that the "best" fish may not be those whose throat colors fall closest to one end of a particular axis through the fish's color space, but rather, or in addition, those whose throat colors most effectively complement iris color.

Throat coloration may have evolved because an iris surrounded by its complementary hue looks more extreme or is more detectable than that same iris without

the surround. A spatial surround's enhancement of its complementary hue (simultaneous color contrast—the fact, that, for instance, a yellow circle in a blue annulus appears more yellow than the same circle in a white annulus) is well known in humans, and seems to characterize the vision of some fish (Dorr and Neumeyer 1997) including *G. aculeatus* (Herter 1950). Consequently, despite the focus of human experimenters on the extent or degree of throat coloration, fish might be responding more to the iris than the throat, and the throat may serve mainly to draw attention to the iris or increase its signal efficacy. Clearly, it is also possible that accentuation of the iris played a role in the early evolution of throat color, and that throat color only later evolved to have signal value independent of the iris. Iris coloration probably preceded throat coloration; iris color is more widely distributed across populations, and the blue is probably cheaper to produce (i.e., it is presumably a structural color and hence does not depend upon foraging ability or costly biochemistry).

The potential signal value of non-spectral characteristics of the iris (e.g., size and shape) suggests a "hue-independent" version of the anti-iris hypothesis. The particular color of the iris may be less important than its detectability under natural illumination and against natural spectral backgrounds—including surrounding body surfaces.

The ordering of evolutionary events

For the most part, we have referred to optimization of the photopigments as though throat reflectances were fixed and selection favored photopigments that make best use of the information provided by throat color. This was merely a convenience because photopigments can be largely specified by two parameters—chromophore type (derivatives of vitamin A_1 or A_2) and λ_{max} (see for example Stavenga et al. 1993). Throat reflectance is more complex because, in principle, the throat reflectance at one region of the spectrum is independent of the reflectance at any other region of the spectrum (e.g., Fig. 2e shows that reflectance between 300 and 400 nm is not necessarily a good predictor of reflectance between 600 and 700 nm). Therefore, it is more difficult to find axes along which throat reflectances vary in order to show that these reflectances are optimized to visual pigments. With the simple manipulation we did try, shifting the reflectance spectra of all male throats to longer or shorter wavelengths without changing their shapes, we found that throat reflectances are within 2 nm of the optimum predicted by the identification/discrimination model. Similarly, if we use the criterion that the optimum throat color is the complement of the iris color, then the throat reflectance distribution is optimized to within 5 nm.

The spectral sensitivity of stickleback photopigments may have constrained the evolution of throat color variation to fall along an axis that maximizes the response in one color opponent mechanism (the proposed discrimination channel) and minimizes the response in a second color opponent mechanism (the proposed identification channel). Alternatively, photopigment spectral sensitivities may have selected for throat colors that enhance the conspicuousness of the iris, which would also constrain the evolution of throat color variation to follow a linear trajectory in stickleback color space. Whether evolution followed one of these two scenarios, or instead photopigments evolved to best extract information from an existing pattern of throat color variation, we would expect to find evidence for optimization such as that reported here.

As argued above, stickleback photoreceptors probably preceded throat coloration in the evolution of each to their present states. However, the processing of the outputs of those receptors may still have evolved along with or in response to the evolution of throat coloration. We suggest that direct anatomical and physiological evidence for or against the channels we've proposed should be sought in *G. aculeatus*. Assuming such channels are found, it would then be instructive to look for similar channels in other gasterosteid fish. Finding such channels in other members of the clade would suggest that male throat coloration evolved to exploit these channels (and/or to maximally accentuate iris color given these channels). Alternatively, finding the proposed channels only in *G. aculeatus*, would suggest that selection has operated on the color processing mechanisms to improve the animals' ability to identify and discriminate among male throat colors.

Applicability to other animals

Our proposal that threespine stickleback identify and discriminate throat colors using independent perceptual mechanisms is similar to the proposal by Ryan and Rand (1995) that female túngara frogs (*Physalaemus pustulatus*) use different perceptual mechanisms to recognize a sound as the call of a potential mate and to discriminate between the calls of conspecific and heterospecific males. If distinguishing between conspecific, and heterospecific, (and hypothetical ancestral) calls is an extension of mate discrimination—i.e., if females respond to heterospecific males as low quality mates—then the independence proposed by Ryan and Rand parallels that of the identification/discrimination model of stickleback throat color assessment. If future experiments—many of which could be carried out with computer animations (Künzler and Bakker 2001) or dummy fish (Rowland 1989)—support the hypothesized identification/discrimination model in threespine stickleback, the likelihood that such mechanisms are a general characteristic of signal/receiver systems that have evolved through sexual selection will be strengthened by the fact that the two sets of findings involve different sensory modalities, phylogenetically distinct vertebrates, and different experimental approaches.

References

Ali MA, Anctil M (1976) Retinas of fishes: an atlas. Springer, Berlin Heidelberg New York

Bakker TC (1993) Positive genetic correlation between female preference and preferred male ornament in sticklebacks. Nature 352:155–156

Baube CL (1994) The perceptual mechanisms of sexual selection in sticklebacks. Ph.D. Thesis, Indiana University, Bloomington, IN

Bennett ATD, Cuthill IC, Norris KJ (1994) Sexual selection and the mismeasure of color. Am Nat 144:848–860

Blouw DM, Hagen DW (1990) Breeding ecology and evidence of reproductive isolation of a widespread stickleback fish (Gasterosteidae) in Nova Scotia, Canada. Biol J Linn Soc 39:195–217

Boughman JW (2001) Divergent sexual selection enhances reproductive isolation in sticklebacks. Nature 411:944–948

Brush AH, Reisman MR (1965) The carotenoid pigments in the three-spined stickleback, *Gasterosteus aculeatus*. Comp Biochem Physiol 14:121–125

Candolin U (2000) Increased signalling effort when survival prospects decrease: male-male competition ensures honesty. Anim Behav 60:417–422

Candolin U, Voigt H-R (2001) No effect of a parasite on reproduction in stickleback males: a laboratory artefact? Parasitology 122:457–464

Chittka L (1992) The colour hexagon: a chromaticity diagram based on photoreceptor excitations as a generalized representation of colour opponency. J Comp Physiol A 170:533–543

Chittka L (1996) Does bee color vision predate the evolution of flower color? Naturwissenschaften 83:136–138

Chittka L (1997) Bee color vision is optimal for coding flower color, but flower colors are not optimal for being coded—why? Isr J Plant Sci 45:115–127

Chittka L, Briscoe A (2001) Why sensory ecology needs to become more evolutionary—insect color vision as a case in point. In: Barth FG, Schmid A (eds) Ecology of sensing. Springer, Berlin Heidelberg New York, pp 19–37

Chittka L, Menzel R (1992) The evolutionary adaptation of flower colours and the insect pollinators' color vision. J Comp Physiol A 171:171–181

Chittka L, Beier W, Hertel H, Steinmann E, Menzel R (1992) Opponent colour coding is a universal strategy to evaluate the photoreceptor inputs in Hymenoptera. J Comp Physiol A 170:545–563

C.I.E. (Commission Internationale de L'Eclairage) (1977) Radiometric and photometric characteristics of materials and their measurement. C.I.E., Paris, France

Cronly-Dillon J R, Sharma SC (1968) Effect of season and sex on the photopic spectral sensitivity of the three-spine stickleback. J Exp Biol 49:679–687

Dorr S, Neumeyer C (1997) Simultaneous color contrast in goldfish—a quantitative study. Vision Res 37:1581–1593

Douglas RH, Marshall NJ (1999) A review of vertebrate and invertebrate optical filters. In: Archer SN, Djamgoz MBA, Loew ER, Partridge JC, Vallerga S (eds) Adaptive mechanisms in the ecology of vision. Kluwer, Boston

Endler JA (1991) Variation in the appearance of guppy color patterns to guppies and their predators under different visual conditions. Vision Res 31:587–608

Endler JA (2000) Evolutionary implications of the interaction between animal signals and the environment. In: Espmark Y, Amundsen T, Rosenqvist G (eds) Animal signals: signalling and signal design in animal communication. Tapir Academic Press, Trondheim, Norway

Fleishman LJ, Endler JA (2000) Some comments on visual perception and the use of video playback in animal behavior studies. Acta Ethol 3:15–27

Fleishman LJ, McClintock WJ, D'eath RB, Brainard DH, Endler JA (1998) Colour perception and the use of video playback experiments in animal behaviour. Anim Behav 56:1035–1040

Gamble S, Lindholm AK, Endler JA, Brooks R (2003) Environmental variation and the maintenance of polymorphism: the effect of ambient light spectrum on mating behaviour and sexual selection in guppies. Ecol Lett 6:463–472

Grether GF, Hudon J, Endler JA (2001) Carotenoid scarcity, synthetic pteridine pigments and the evolution of sexual coloration in guppies (*Poecilia reticulata*). Proc R Soc London Ser B 268:1245–1253

Heiling AM, Herberstein, ME, Chittka L (2003) Crab-spiders manipulate flower signals. Nature 421:334

Herter K (1950) Über simultanen Farbkontrast bei Fischen. Z Vergl Physiol 60:283–300

Houde AE, Endler JA (1990) Correlated evolution of female mating preferences and male color patterns in the guppy *Poecilia reticulata*. Science 248:1405–1408

Hunt DM, Dulai KS, Cowing JA, Julliot C, Mollon JD, Bowmaker JS, Li W-H, Hewett-Emmett D (1998) Molecular evolution of trichromacy in primates. Vision Res 38:3299–3306

Kokko H (1998) Should advertising parental care be honest? Proc R Soc London Ser B 265:1871–1878

Künzler R, Bakker TCM (2001) Female preferences for single and combined traits in computer animated stickleback males. Behav Ecol 12:681–685

Lipetz LE, Cronin TW (1988) Application of an invariant spectral form to the visual pigments of crustaceans—implications regarding the binding of the chromophore. Vision Res 28:1083–1093

Loew ER (1994) A third, ultraviolet-sensitive, visual pigment in the tokay gecko (*Gekko gekko*). Vision Res 34:1427–1431

Lythgoe JN (1979) The ecology of vision. Clarendon Press, Oxford

Lythgoe JN, Partridge JC (1989) Visual pigments and the acquisition of visual information. J Exp Biol 146:1–20

MacNichol EF (1986) A unifying presentation of photopigment spectra. Vision Res 26:1543–1556

Milinski M, Bakker TCM (1990) Female sticklebacks use male coloration in mate choice and hence avoid parasitized males. Nature 344:330–333

Mollon JD (1989) "Tho' she kneel'd in that place where they grew.." the uses and origins of primate color vision. J Exp Biol 146:21–38

Naka KJ, Rushton WAH (1966) S-potentials from colour units in the retina of fish (Cyprinidae). J Physiol (Lond) 185:536–555

Normann RA, Werblin FS (1974) Control of retinal sensitivity. I. light and dark-adaptation of vertebrate rods and cones. J Gen Physiol 63:37–61

Osorio D, Vorobyev M (1996) Colour vision as an adaptation to frugivory in primates. Proc R Soc London Ser B 263:593–599

Östland Nilsson S, Nilsson GE (2000) Free choice by female sticklebacks: lack of preference for male dominance traits. Can J Zool 78:1251–1258

Palacios AG, Varela FJ, Srivastava R, Goldsmith T (1998) Spectral sensitivity of cones in the goldfish, *Carassius auratus*. Vision Res 38:2135–2146

Press WH, Flannery BP, Teukolsky SA, Vetterling WT (1987) Numerical recipes in Pascal. Cambridge University Press, Cambridge

Regan BC, Julliot C, Simmen B, Viénot F, Charles-Dominique P, Mollon JD (1998) Frugivory and colour vision in *Alouatta seniculus*, a trichromatic platyrrhine monkey. Vision Res 38:3321–3327

Reimchen TE (1989) Loss of nuptial color in threespine sticklebacks (*Gasterosteus aculeatus*). Evolution 43:450–460

Rowland WJ (1989) Mate choice and supernormality effect in female sticklebacks (*Gasterosteus aculeatus*). Behav Ecol Sociobiol 24:433–438

Rowland WJ (1994) Proximate determinants of stickleback behaviour: an evolutionary perspective. In: Bell MA, Foster SA (eds) The evolutionary biology of the threespine stickleback. Oxford University Press, New York

Ryan MJ, Rand AS (1995) Female responses to ancestral advertisement calls in túngara frogs. Science 269:390–392

Sernagor E, Eglen SJ, Wong ROL (2001) Development of retinal ganglion cell structure and function. Prog Retin Eye Res 20:139–174

Shapley RJ, Enroth-Cugell C (1984) Visual adaptation and retinal gain controls. Prog Retin Eye Res 3:263–346

Simpson KL, Katayama T, Cichester CO (1981) Carotenoids in fish feeds. In: Bauernfeind JC (ed) Carotenoids as colorants and vitamin a precursors: technological and nutritional applications. Academic Press, New York

Smith AC, Buchanan-Smith HM, Surridge AK, Osorio D, Mundy NI (2003) The effect of colour vision status on the detection and selection of fruits by tamarins (*Saguinus* spp.). J Exp Biol 206:3159–3165

Stavenga DG, Smits RP, Hoenders BJ (1993) Simple exponential functions describing the absorbance bands of visual pigment spectra. Vision Res 33:1011–1017

Ter Pelkwijk JJ, Tinbergen N (1937) Eine reizbiologische Analyse einiger Verhaltensweisen von *Gasterosteus aculeatus*, L. Z Tierpsychol 1:193–200

Wedekind C, Meyer P, Frischknecht M, Niggli UA, Pfander H (1998) Different carotenoids and potential information content of red coloration of male three-spined stickleback. J Chem Ecol 24:787–801